

RESEARCH ARTICLE

Pharmacokinetic, pharmacodynamic, and transcriptomic analysis of chronic levetiracetam treatment in 5XFAD mice: A MODEL-AD preclinical testing core study

Kristen D. Onos¹ | Sara K. Quinney² | David R. Jones² | Andrea R. Masters² | Ravi Pandey¹ | Kelly J. Keezer¹ | Carla Biesdorf² | Ingrid F. Metzger² | Jill A. Meyers² | Johnathon Peters² | Scott C. Persohn² | Brian P. McCarthy² | Amanda A. Bedwell² | Lucas L. Figueiredo² | Zackary A. Cope³ | Michael Sasner¹ | Gareth R. Howell¹ | Harriet M. Williams¹ | Adrian L. Oblak² | Bruce T. Lamb² | Gregory W. Carter¹ | Stacey J. Sukoff Rizzo³ | Paul R. Territo²

¹The Jackson Laboratory, Bar Harbor, Maine, USA

²Indiana University School of Medicine, Indianapolis, Indiana, USA

³University of Pittsburgh, Pittsburgh, Pennsylvania, USA

Correspondence

Kristen D. Onos, The Jackson Laboratory, 600 Main Street, Bar Harbor, ME 04609, USA.

E-mail: Kristen.Onos@jax.org

Abstract

Introduction: Hyperexcitability and epileptiform activity are commonplace in Alzheimer's disease (AD) patients and associated with impaired cognitive function. The anti-seizure drug levetiracetam (LEV) is currently being evaluated in clinical trials for ability to reduce epileptiform activity and improve cognitive function in AD. The purpose of our studies was to establish a pharmacokinetic/pharmacodynamic (PK/PD) relationship with LEV in an amyloidogenic mouse model of AD to enable predictive preclinical to clinical translation, using the rigorous preclinical testing pipeline of the Model Organism Development and Evaluation for Late-Onset Alzheimer's Disease Preclinical Testing Core.

Methods: A multi-tier approach was applied that included quality assurance and quality control of the active pharmaceutical ingredient, PK/PD modeling, positron emission tomography/magnetic resonance imaging (PET/MRI), functional outcomes, and transcriptomics. 5XFAD mice were treated chronically with LEV for 3 months at doses in line with those allometrically scaled to the clinical dose range.

Results: Pharmacokinetics of LEV demonstrated sex differences in C_{max} , $AUC_{0-\infty}$, and CL/F , and a dose dependence in $AUC_{0-\infty}$. After chronic dosing at 10, 30, 56 mg/kg, PET/MRI tracer ^{18}F -AV45, and ^{18}F -fluorodeoxyglucose (^{18}F -FDG) showed specific regional differences with treatment. LEV did not significantly improve cognitive outcomes. Transcriptomics performed by nanoString demonstrated drug- and dose-related changes in gene expression relevant to human brain regions and pathways congruent with changes in ^{18}F -FDG uptake.

This is an open access article under the terms of the [Creative Commons Attribution-NonCommercial-NoDerivs](https://creativecommons.org/licenses/by-nc-nd/4.0/) License, which permits use and distribution in any medium, provided the original work is properly cited, the use is non-commercial and no modifications or adaptations are made.

© 2022 The Authors. *Alzheimer's & Dementia: Translational Research & Clinical Interventions* published by Wiley Periodicals LLC on behalf of Alzheimer's Association.

Discussion: This study represents the first report of PK/PD assessment of LEV in 5XFAD mice. Overall, these results highlighted non-linear kinetics based on dose and sex. Plasma concentrations of the 10 mg/kg dose in 5XFAD overlapped with human plasma concentrations used for studies of mild cognitive impairment, while the 30 and 56 mg/kg doses were reflective of doses used to treat seizure activity. Post-treatment gene expression analysis demonstrated LEV dose-related changes in immune function and neuronal-signaling pathways relevant to human AD, and aligned with regional ¹⁸F-FDG uptake. Overall, this study highlights the importance of PK/PD relationships in preclinical studies to inform clinical study design.

KEYWORDS

Alzheimer's disease, levetiracetam, preclinical testing, 5XFAD

Highlights

- Significant sex differences in pharmacokinetics of levetiracetam were observed in 5XFAD mice.
- Plasma concentrations of 10 mg/kg levetiracetam dose in 5XFAD overlapped with human plasma concentration used in the clinic.
- Drug- and dose-related differences in gene expression relevant to human brain regions and pathways were also similar to brain region-specific changes in ¹⁸F-fluorodeoxyglucose uptake.

1 | INTRODUCTION

Levetiracetam (LEV) was approved by the Food and Drug Administration in 2000 for the treatment of seizures and long-term epilepsy in adults and children.¹ Observational studies in Alzheimer's disease (AD) patients prescribed LEV for the treatment of co-morbid seizures reported improved cognition as determined by Alzheimer's Disease Assessment Scale–Cognitive subscale and Mini-Mental State Examination testing.^{2,3} A number of clinical trials studying LEV in AD patients are ongoing, some of which are investigating the use of an extended release form of LEV, known as AGB101.⁴ The working hypotheses of these trials is that hippocampal hyper-excitability is a pathophysiological mechanism underlying cognitive dysfunction in mild cognitive impairment (MCI) that predisposes subjects to AD.⁵ This hippocampal excitability has also been demonstrated in apolipoprotein E $\epsilon 4/\epsilon 4$ carriers,⁶ the greatest genetic risk factor for late-onset AD (LOAD), which suggests that LEV may not only be useful for interventional use with early-onset AD, but also as a prophylactic in treatment of LOAD.⁶

While the mechanism of action of LEV in AD is not fully understood, it is known to modulate synaptic neurotransmitter release through binding to a synaptic vesicle glycoprotein 2A (SV2A).^{1,7} Neuromodulation through SV2A has been suggested to occur through inhibition of presynaptic calcium channels, lowering impulse conduction and enhancing selectivity low-frequency neurotransmission.⁸ In initial phases of drug repurposing of LEV for MCI, it was determined

that effectiveness was non-dose proportionate.^{2,9–11} For instance, one study that tested patients with MCI and controls using functional magnetic resonance imaging (MRI) on a memory task found that low (62.5 mg BID) and medium (125 mg BID) doses of LEV restored abnormal hippocampal activity in the dentate gyrus/CA3 regions, and participants showed improvement in performance; however, effectiveness was lost at higher doses (250 mg BID), and hippocampal activity appeared to lose synchronicity.⁹

Clinically, hyper-excitability has been linked to seizure activity in AD subjects,^{3,12,13} and this has been replicated in current mouse models of AD such as 5XFAD and *APP/PS1*.^{14,15} Acute treatment with LEV in amyloid mouse models has shown restoration of abnormal spike activity,¹⁴ while chronic treatment via continuous infusion via minipumps has been associated with the reversal of synaptic loss and behavioral impairment in hAPP mice.¹⁶ These preclinical studies, however did not fully characterize the pharmacokinetic/pharmacodynamic (PK/PD) relationship of LEV, which is critically important for predicting the type of non-dose proportionate efficacy observed in the clinic. Notably, LEV dosed once per day may not be sufficient to maintain exposure levels and minimize C_{\min}/C_{\max} ratios.

The purpose of the present studies was to establish a PK/PD relationship of LEV in a mouse model of AD that could be used to better predict clinical efficacy. We evaluated LEV using the recently established resources of the Model Organism Development and Evaluation for Late-Onset Alzheimer's Disease (MODEL-AD) Preclinical Testing Core (PTC). The PTC focused on determination of the PK

profile of LEV in the widely used 5XFAD mouse model at an age when significant AD pathology is observed, permitting the appropriate dose levels, frequency, and duration for chronic dosing studies. PD assessment followed chronic 3-month administration, and was comprised of ^{18}F -AV45 and ^{18}F -fluorodeoxyglucose (^{18}F -FDG) positron emission tomography (PET)/MRI to assess differences in amyloid deposition and glucose uptake as translational surrogate biomarkers for region-specific drug efficacy. Previous work has highlighted an interrelationship between brain metabolism and amyloid deposition, particularly in MCI patients.^{17,18} Furthermore, early stages of AD are associated with neuronal hyperactivity, and this has been suggested to either be triggered by accumulation of soluble amyloid beta oligomers, or lead to their increased production.^{19–21} Cognitive and behavioral profiling followed LEV treatment to determine the potential side effect profile and therapeutic window of LEV; finally, transcriptional profiling using nanoString was performed to determine the drug effects at a molecular level.

2 | METHODS

All studies followed the Animal Research: Reporting of In Vivo Experiments (ARRIVE) guidelines¹ and were approved by the Institutional Animal Use and Care Committees (IACUC) at each respective site. For a detailed description of the materials and procedures, please refer to the supporting information.

2.1 | Housing conditions and cohort generation at Indiana University

Adult male and female 5XFAD mice, and non-transgenic wild-type (WT) controls were bred at Indiana University (IU) by crossing male 5XFAD mice (JAX MMRRC stock #: 34848) to female C57BL6/J (JAX MMRRC stock #: 000664). Animals were housed up to five per cage with SaniChip bedding and remained group housed during dosing studies. The colony room was kept on a 12:12 light:dark schedule (lights on at 6:00 am). Two separate cohorts were enrolled for the respective endpoints of ^{18}F -AV-45 and ^{18}F -FDG-PET.

2.2 | Housing conditions and cohort generation at The Jackson Laboratory

Adult male and female 5XFAD mice and non-transgenic WT controls were bred at The Jackson Laboratory (JAX) using the same methods described for IU. Initially, animals were housed up to five per side in duplex cages with pine bedding. The colony room was kept on a 12:12 light:dark schedule. For chronic dosing studies, an $n = 10$ to 15 subjects per sex per treatment were enrolled into the study, with treatment and sex randomized across two cohorts that were staggered 4 weeks apart ($n = 5–8$ per sex per treatment per cohort). One week prior to study start, subjects were individually housed and

RESEARCH IN CONTEXT

- 1. Systematic Review:** The authors reviewed the literature using traditional sources (e.g., PubMed) and databases (e.g., ClinicalTrials.gov) to assess the status of levetiracetam (LEV) in clinical trials for Alzheimer's disease (AD) and in preclinical studies in animal models. To our knowledge there have been limited data using pharmacokinetic/pharmacodynamic (PK/PD) modeling in animal models of AD, which is to inform clinical trials of LEV in AD patients.
- 2. Interpretation:** Rigorous preclinical drug screening conducted by the Model Organism Development and Evaluation for Late-Onset Alzheimer's Disease Preclinical Testing core for LEV treatment in 5XFAD mice revealed non-linear kinetics, sex differences, and no significant changes in amyloid deposition or improvements in cognitive function. However, allometric scaling to the clinical dose range implicated important PK/PD relationships related to changes in ^{18}F -fluorodeoxyglucose positron emission tomography and in gene expression. Gene expression differences in LEV-treated 5XFAD mice were determined via the nanoString Mouse AD Panel, and correlated with human AD gene expression changes in specific brain regions.
- 3. Future Directions:** Establishing a PK/PD relationship in preclinical studies may provide better predictions for informing preclinical to clinical translation relative to traditional drug screening approaches in animal models. Furthermore, assessment of LEV in newly developed LOAD mouse models may align with ongoing clinical trials in AD patient populations that do not demonstrate seizure activity, or carry early-onset gene mutations.

were transported to a colony room adjacent to the behavioral testing facility.

2.3 | Levetiracetam pharmacokinetic studies

In vivo PK sampling for LEV was initially conducted at JAX following dosing and serial sampling in 6-month aged male and female 5XFAD mice. LEV (Sigma # L8668-100 mg; Lot # 051M4742V) was dissolved in sterile saline (vehicle) at a concentration of 10 mg/ml and serially diluted with saline to produce concentrations of 3 mg/ml and 1 mg/ml. Six-month aged 5XFAD mice ($n = 3$ per dose per sex) were dosed 10, 30, and 100 mg/kg (10 ml/kg dose volume). Serial plasma samples were collected via tail vein prior to dosing and at 0.25, 0.5, 1, 2, 4, 6, and 24 hours after dosing. Mice were euthanized at 24 hours at which time brain cortex tissue was excised, frozen on dry ice, and stored at -80°C

until shipped to IU for LEV quantification and PK analysis of plasma and tissue concentrations.

2.4 | Levetiracetam quantification

LEV and ECA (Etiracetam) concentrations were determined using liquid chromatography tandem mass spectrometry (LC-MS/MS), with TMP (Temazepam) as an internal standard, using an Agilent 1290 UHPLC, Eskigent Autosampler, and Sciex 5500 QTRAP. Standard curves ranged from 0.3–30000 ng/mL for plasma and 0.8–800 ng/g in brain homogenate. The inter-day precision ranged from 5.3% to 15.4% for LEV and 10.7% to 17.0% for ECA. The inter-day accuracy ranged from 88.1% to 108.0% for LEV and 88.4% to 103.0% for ECA. Inter-day variability was only performed for plasma matrix due to limited resources of naïve brains.

2.5 | Pharmacokinetic modeling

PK parameters were estimated using standard noncompartmental analysis (NCA) using WinNonlin (Phoenix 64, build 8.0.0.3176). Terminal slopes were automatically calculated using linear regression with uniform weighting, with visual verification. Area under the curve (AUC_{0-t} , $AUC_{0-\infty}$) were estimated using the linear trapezoidal/linear interpolation option. Chronic-dosing plasma and brain concentrations were predicted using a 2-stage approach by fitting individual LEV plasma versus time data to a one-compartment model. Models were evaluated based on visual inspection of fits, residual plots, appropriateness of parameter estimates, and Akaike information criterion metrics.²²

2.6 | Chronic dosing simulations

Simulations of chronic dosing schedules were conducted using the deSolve²³ package in R (v3.4.3)²⁴ through the RStudio graphical user interface (v1.1.423) using a first-order absorption, one compartment model, which was found to best fit the single dose data:

$$\frac{dC_p}{dt} = \frac{Ag \times ka - A \times ke}{V/F} \quad (1)$$

where, Ag , F , V , k_a , and k_e are the amount of drug in the gut ($Ag_0 = \text{Dose}$), bioavailability, volume of distribution, absorption rate constant, and elimination rate constant, respectively.

2.7 | Brain to plasma ratio

Cerebellum and cortex concentrations of drug in brain were obtained with the terminal PK time point, and assessed to determine the tissue to plasma partition coefficient.

2.8 | Drug administration for chronic studies

Animals were weighed each morning, and dosed twice daily (BID) for 3 months (7:00–9:00 am and 3:00–5:00 pm) via oral gavage (10 ml/kg dose volume), where LEV (SelleckChem # S1356, bulk lot # S135602) was formulated in saline once weekly, and vials blinded with A, B, C, and D (JAX) or Blue, Red, Yellow, and Green (IU). The Clinical Pharmacology Analytical Core confirmed stability of drug formulation over a 1-week period. On each behavioral testing day, the pretreatment time of LEV dosing was 30 minutes prior to testing. During chronic dosing, animals were closely monitored for any indication of toxicology or drug related side effects. Attrition ($n = 13$) at JAX occurred equally across all dose levels and genotypes. For cases outside of dermatitis, necropsy confirmed animals showed pathological signs of pneumonia in the lungs. Attrition ($n = 3$) at IU was lower, was not specific to a dose level, and occurred either due to dermatitis or lung puncture during oral gavage.

2.9 | Terminal tissue collection

At the conclusion of behavioral testing, terminal CSF, plasma, and brain tissue were collected under isoflurane anesthesia after a final dose of LEV with a pretreatment time of 30 minutes. Bioanalytical analysis was performed by LC-MS/MS and terminal plasma and right brain hemisphere for confirmatory PK. Transcriptional profiling: Homogenate from left brain hemisphere was analyzed using a custom nanoString nCounter[®] Mouse AD panel that was designed to identify correlations to changes in gene expression specific to clinical LOAD. Differential gene expression was determined based on genotype, sex, and treatment.

2.10 | Rigor and reproducibility

All technicians were blinded to genotype and drug dose during study execution and through data analysis in accordance with the ARRIVE guidelines.²⁵

3 | RESULTS

3.1 | Pharmacokinetic study results

Initial PK work conducted on male and female 6-month 5XFAD mice indicated that LEV exhibited nonlinear clearance, leading to differences in dose-corrected C_{max} and $AUC_{0-\infty}$, and showed a statistically significant effect of sex on both apparent volume of distribution and oral clearance (Table 1, Figure 1A-C). However, these sex-specific differences disappeared at the 100 mg/kg dose of LEV (Figure 1C). Mean half-life was 2.7 ± 0.56 hours (Table 1). PK modeling demonstrated that minimum therapeutic concentrations of LEV could be maintained in plasma and brain at doses as low as 10 mg/kg twice daily (Figure 1D).

TABLE 1 Noncompartmental pharmacokinetics

	10 mg/kg		30 mg/kg		100 mg/kg	
	Female	Male	Female	Male	Female	Male
Levetiracetam						
ke (1/h)	0.30 ± 0.12	0.21 ± 0.03	0.26 ± 0.02	0.25 ± 0.03	0.29 ± 0.07	0.27 ± 0.02
Half-life (h)	2.53 ± 0.84	3.31 ± 0.37	2.72 ± 0.25	2.76 ± 0.30	2.52 ± 0.57	2.54 ± 0.22
Tmax (h)	0.86 ± 0.24	0.85 ± 0.28	0.86 ± 0.29	0.84 ± 0.30	0.51 ± 0.45	0.44 ± 0.14
Cmax (μg/L) ^a	8.10 ± 1.80	3.50 ± 0.73	16.1 ± 1.23	12.4 ± 1.80	28.7 ± 1.60	35.0 ± 2.35
AUCinf (mg/L/h) ^a	28.2 ± 5.50	15.1 ± 5.10	59.7 ± 13.4	44.0 ± 14.5	110 ± 9.31	113 ± 9.09
Vd/F (L/kg) ^a	1.33 ± 0.55	3.45 ± 1.27	2.06 ± 0.61	3.06 ± 1.59	3.37 ± 1.03	3.24 ± 0.02
CL/F (L/h/kg) ^a	0.36 ± 0.07	0.71 ± 0.20	0.52 ± 0.13	0.75 ± 0.31	0.91 ± 0.08	0.89 ± 0.07
Etiracetam						
ke (1/h)	0.23 ± 0.14	0.25 ± 0.24	0.19 ± 0.004	0.19 ± 0.16	0.31 ± 0.15	0.23 ± 0.18
Half-life (h)	3.84 ± 1.91	6.05 ± 6.19	3.68 ± 0.08	5.54 ± 3.89	2.56 ± 1.07	4.43 ± 2.83
Tmax (h)	0.86 ± 0.29	2.36 ± 1.51	1.35 ± 0.56	0.85 ± 0.28	1.03 ± 0.01	0.85 ± 0.28
Cmax (μg/L) ^a	136 ± 43.4	87.7 ± 9.50	367 ± 103	250 ± 25.8	902 ± 167	559 ± 106
AUCinf (μg/L/h) ^b	591 ± 209	1256 ± 568	1483 ± 510	1729 ± 489	2847 ± 639	3620 ± 1236

^aSignificant differences between males and females and dose levels ($P < .05$, 2-way ANOVA) after correcting C_{max} and AUC for dose.

^bSignificant differences between dose levels ($P < .05$, 2-way ANOVA).

Abbreviations: ANOVA, analysis of variance; AUC, area under the curve.

These data led to the selection of 10, 30, and 56 mg/kg being administered via oral gavage BID for the 3-month chronic treatment studies. Clinically, AD patients demonstrating seizure activity are treated with between 500 and 1000 mg BID, while MCI patients have been tested with doses ranging from 62.5 to 125 mg BID, or 220 mg once daily of the extended release AGB101.²⁶ Provided these doses, and the structural model (Equation 1, Figure 1B), an allometric comparison was made with clinically observed concentrations of LEV (Figure 1E), where the gray shaded area indicates the range of plasma concentrations of LEV in clinical studies of MCI patients. These data indicate that only the trough of the 10 mg/kg dose overlaps with this range, while both 30 and 56 mg/kg doses result in plasma concentrations that exceed those observed in MCI studies, and instead are representative of concentrations observed in patients treated with higher doses of LEV for seizure activity. Last, comparison of terminal cortical and plasma concentrations of LEV after 3 months of twice-daily dosing (measured 30 minutes after final dose) shows a linear relationship with daily dose, with female mice showing greater variability than male 5XFAD (Figure 1F). The brain cortex to plasma concentration ratio of LEV was 0.53 ± 0.3 .

3.2 | Neuroimaging with amyloid and glucose PET

To determine the dynamic range of beta amyloid, 6-month WT and 5XFAD mice were scanned with ¹⁸F-AV45 PET/MRI. Significant binding of the tracer was observed in 5XFAD, but not in WT animals, yielding a contrast window which was 2-fold between genotypes. For chronic LEV treatment studies, quantitative analysis of ¹⁸F-AV45 PET/MRI uptake in male and female 5XFAD mice was performed as

a function of dose (Figure 2A). Of the 27 regions studied, principal component analysis (PCA) identified 15 regions that explained 80% of variance in ¹⁸F-AV45 uptake (Figure S1 in supporting information). Analysis of variance (ANOVA) was performed on these regions and a significant difference in uptake of ¹⁸F-AV45 was identified in two regions, secondary somatosensory cortex ($P = .023$) and temporal association cortex ($P = .031$; Figure 2B,C). This significant difference was present dependent on sex only at the 10 mg/kg dose. Staining with ThioS was performed on brain sections to confirm region-specific differences in amyloid deposition (Figure S2 in supporting information) and no significant differences based upon dose were observed.

Like ¹⁸F-AV45, dynamic range of ¹⁸F-FDG in the 5XFAD model was determined in a study of WT and 5XFAD mice,²⁷ and was shown to be 1.5-fold between genotypes (Figure 3A). Using the same PCA approach, 12 of the 27 regions studied explained 80% of variance in ¹⁸F-FDG uptake (Figure S3 in supporting information). ANOVA performed on these regions identified significant sex by dose interactions in the agranular insular cortex ($P = .045$), dysgranular insular cortex ($P = .036$), and secondary motor cortex ($P = .043$; Figure 3B,C).

3.3 | Functional testing

Chronic administration with LEV produced dose-related hyperactivity in 6-month aged 5XFAD male and female mice relative to vehicle-treated 5XFAD and vehicle-treated WT controls in the open field as measured by cumulative distance traveled (Figure 4A). High dose-treated male 5XFAD traveled a significantly higher distance than vehicle-treated WT males ($P = .03$). Chronic administration with LEV

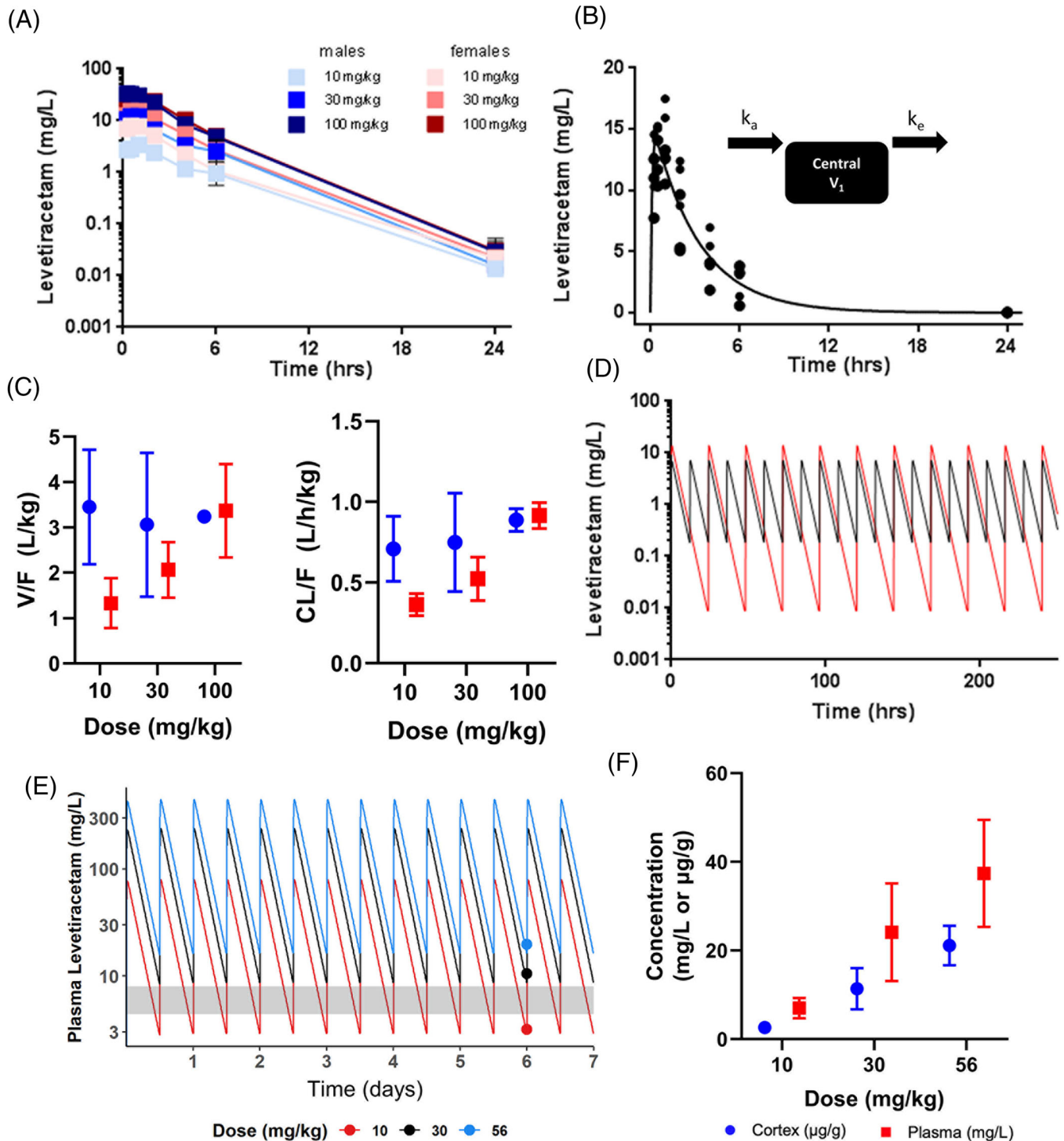


FIGURE 1 Pharmacokinetic analysis of levetiracetam (LEV) in 6-month aged 5XFAD mice reveals significant sex differences. A, Plasma concentration time profiles of LEV by dose and sex in 5XFAD males and females. B, One-compartment model fit for the 30 mg/kg dose. C, Volume of distribution (V/F) and clearance (CL/F) is shown. CL/F is significantly different in male and female 5XFAD ($P = .009$) and LEV dose dependent ($P = .049$) mice. D, Predicted concentration versus time curves for BID (black) and SID (red) dosing. E, Allometric scaling of each dose in relation to LEV doses used in MCI clinical trials. Dots are actual measured concentrations on that day (C_{min} or C_{trough}). Upper part of gray band is long-lasting ABG101, and lower part of band is steady state concentration for single dose of LEV at 125 mg/kg. F, Concentration of LEV in plasma and brain. While exhibiting a linear relationship, there is more variability in female mice

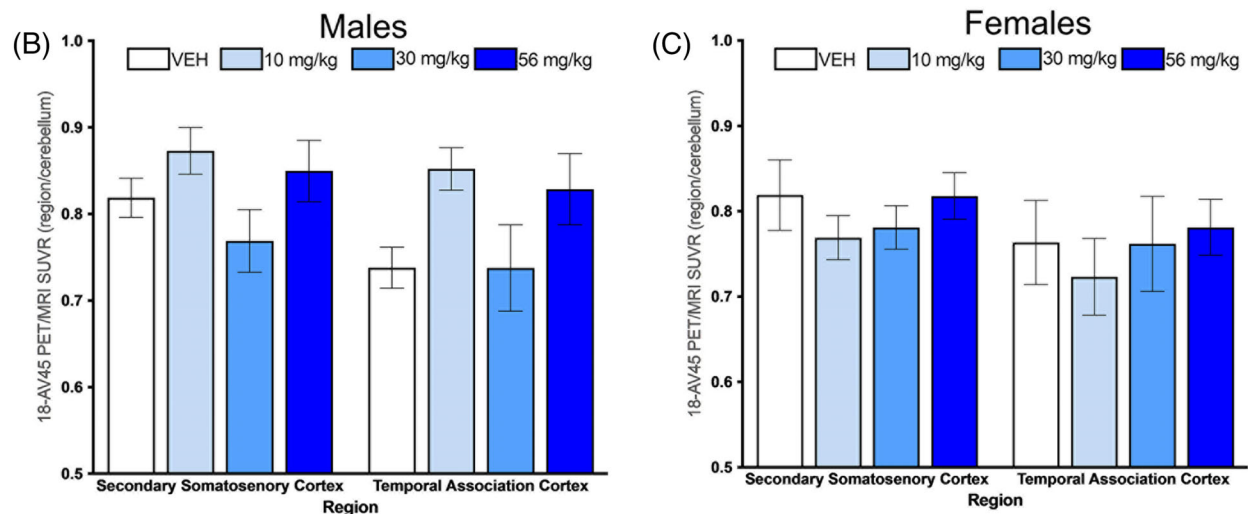
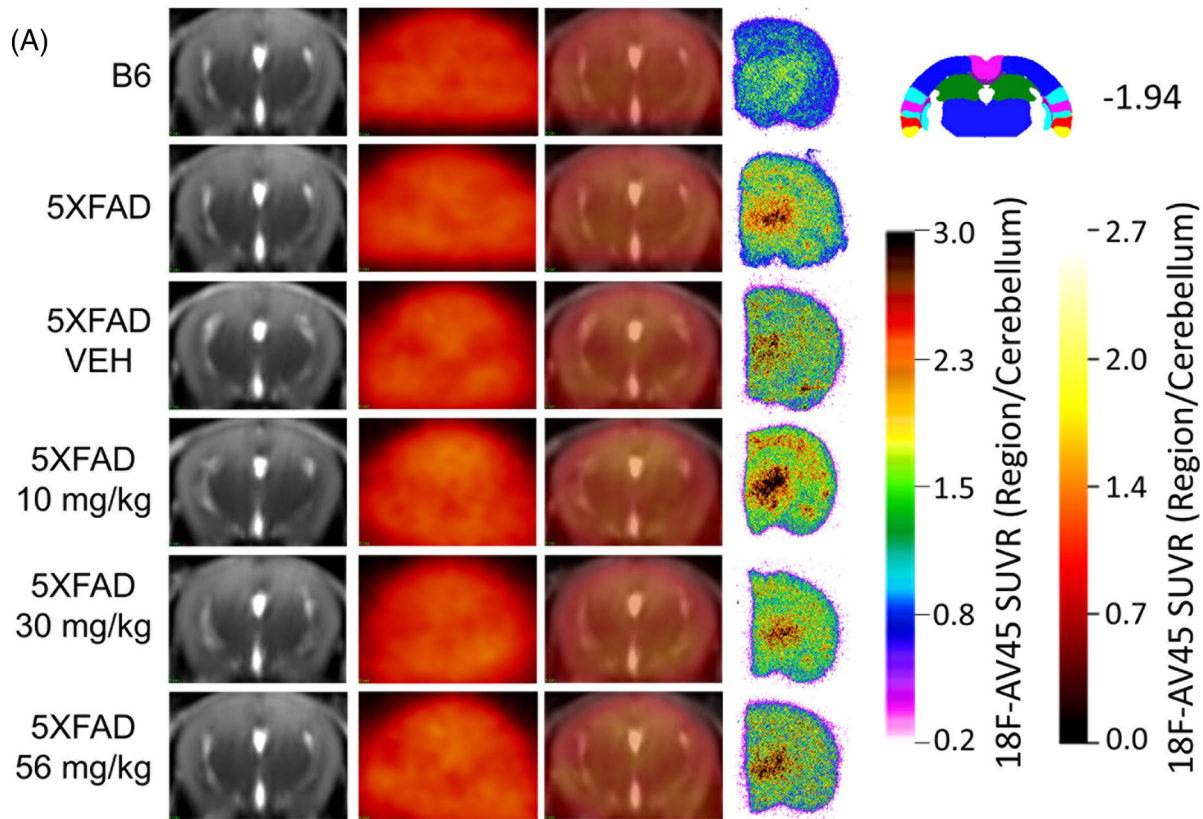


FIGURE 2 ^{18}F -AV45 imaging. (A) Average magnetic resonance imaging (MRI; first column), average positron emission tomography (PET; second column), average fused MRI/PET images (third column), and representative Autorad (fourth column) are presented. The top two rows of images (B6 and 5XFAD) were collected prior to the study. The remaining rows demonstrate all levetiracetam (LEV) treatment groups for the chronic study. B,C, Standardized uptake value ratio referenced to cerebellum in brain regions in which analysis of variance identified a significant difference in signal

did not alter the increase in latency of 5XFAD to maintain their balance on the rotarod relative to WT controls (Figure 4B). Spontaneous alternation was used to assess working memory. While no effect of LEV treatment was observed in male 5XFAD mice, differences were present in female 5XFAD. High dose-treated 5XFAD females performed significantly better than vehicle-treated female 5XFAD ($P = .01$; Figure 4C).

3.4 | nanoString gene expression profiling

Brain hemispheres were assessed via nanoString for gene expression differences using a panel based on human AD gene expression changes.²⁸⁻³² Linear regression analysis revealed genes that were significant at $P < .05$ for genotype, sex, and/or treatment (Figure 5). *Ehfd1*, *Prickle1*, and *Sox8* demonstrated significant dose-specific effects,

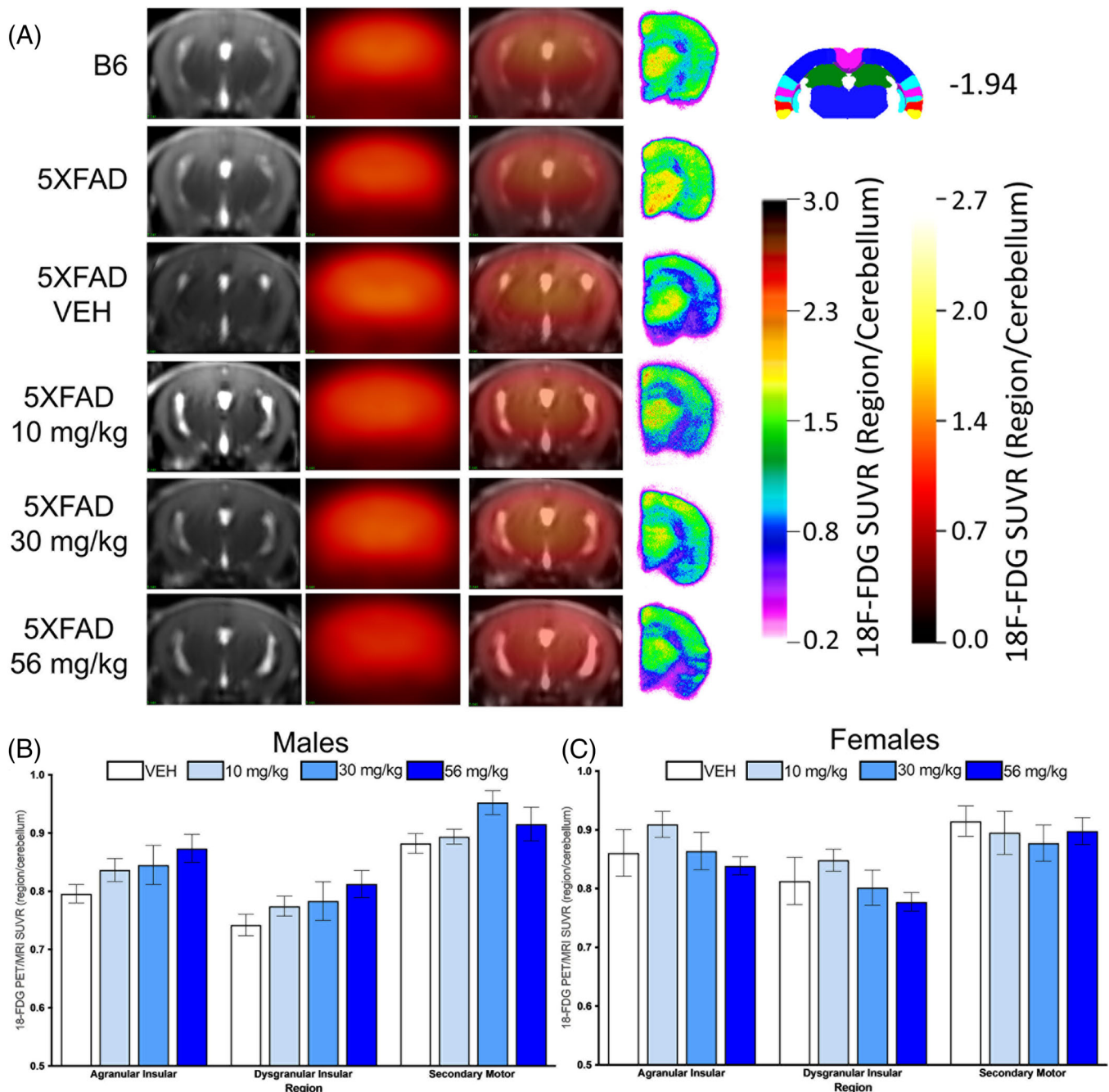


FIGURE 3 ^{18}F -fluorodeoxyglucose (FDG) imaging. A, Average magnetic resonance imaging (MRI; first column), average positron emission tomography (PET; second column), average fused MRI/PET images (third column), and representative AutoRad (fourth column) are presented. The top two rows of images (B6 and 5XFAD) were collected prior to the study. The remaining rows demonstrate all levetiracetam (LEV) treatment groups for the chronic study. B,C, Standardized uptake value ratio referenced to cerebellum in brain regions in which analysis of variance identified a significant difference in signal

though not always in the same direction. *Stat3* demonstrated a dose, sex, and genotype effect (Figure 5A–D).

Data were examined separated by sex and dose levels and expression compared to previously defined Accelerating Medicines Partnership Program for Alzheimer's Disease (AMP AD) consensus clusters.²⁸ A positive correlation between gene expression from the mice in our study with the human consensus cluster demonstrates that the changes in mice match those in humans. A negative correlation

between gene expression between the mice and the human consensus cluster suggests that opposite changes are occurring, and in some cases this may be indicative of resilience or a treatment effect. Overall, the vehicle-treated male and female 5XFAD mice showed significant positive correlations ($P < .05$) with human co-expression modules in Consensus Cluster B that are enriched for immune-related pathways and Consensus Cluster C modules that are enriched for neuronal system-related pathways (Figure 5E,F). Importantly, the

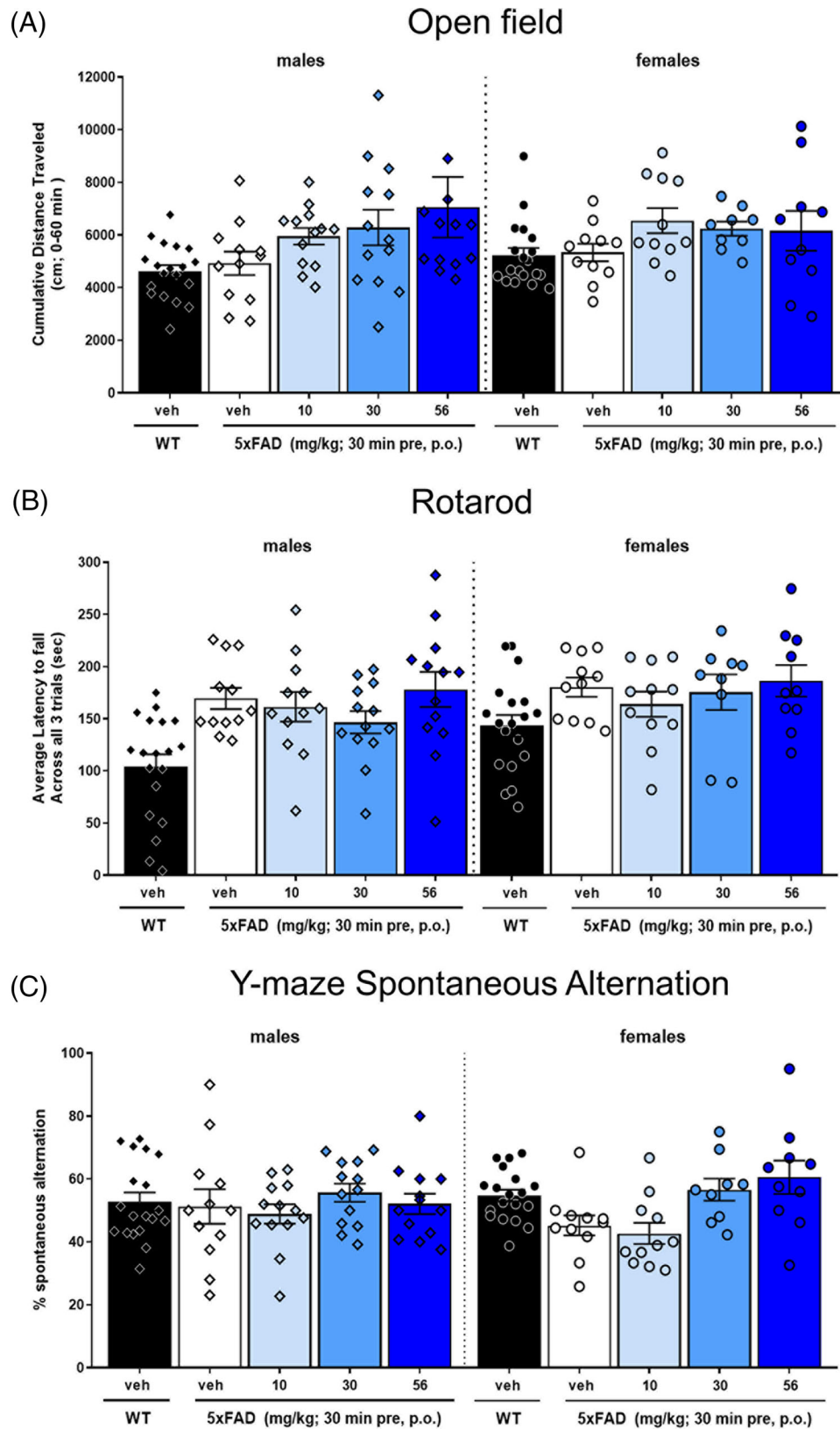


FIGURE 4 Behavioral profiling after chronic treatment of levetiracetam (LEV) in 5XFAD mice (10–56 mg/kg PO, BID). A, Cumulative distance traveled across 60 minutes in the open field arena for vehicle and LEV dose groups. In male animals, high dose-treated 5XFAD males traversed the open field significantly more than vehicle-treated wild-type animals. B, The average latency to fall on the rotarod task across vehicle and dose groups. No significant difference was observed. C, Performance in the spontaneous alternation Y-maze task. No difference was observed in male mice. Female 5XFAD showed a dose-related difference in performance, with high dose-treated 5XFAD performing better than vehicle treated 5XFAD mice

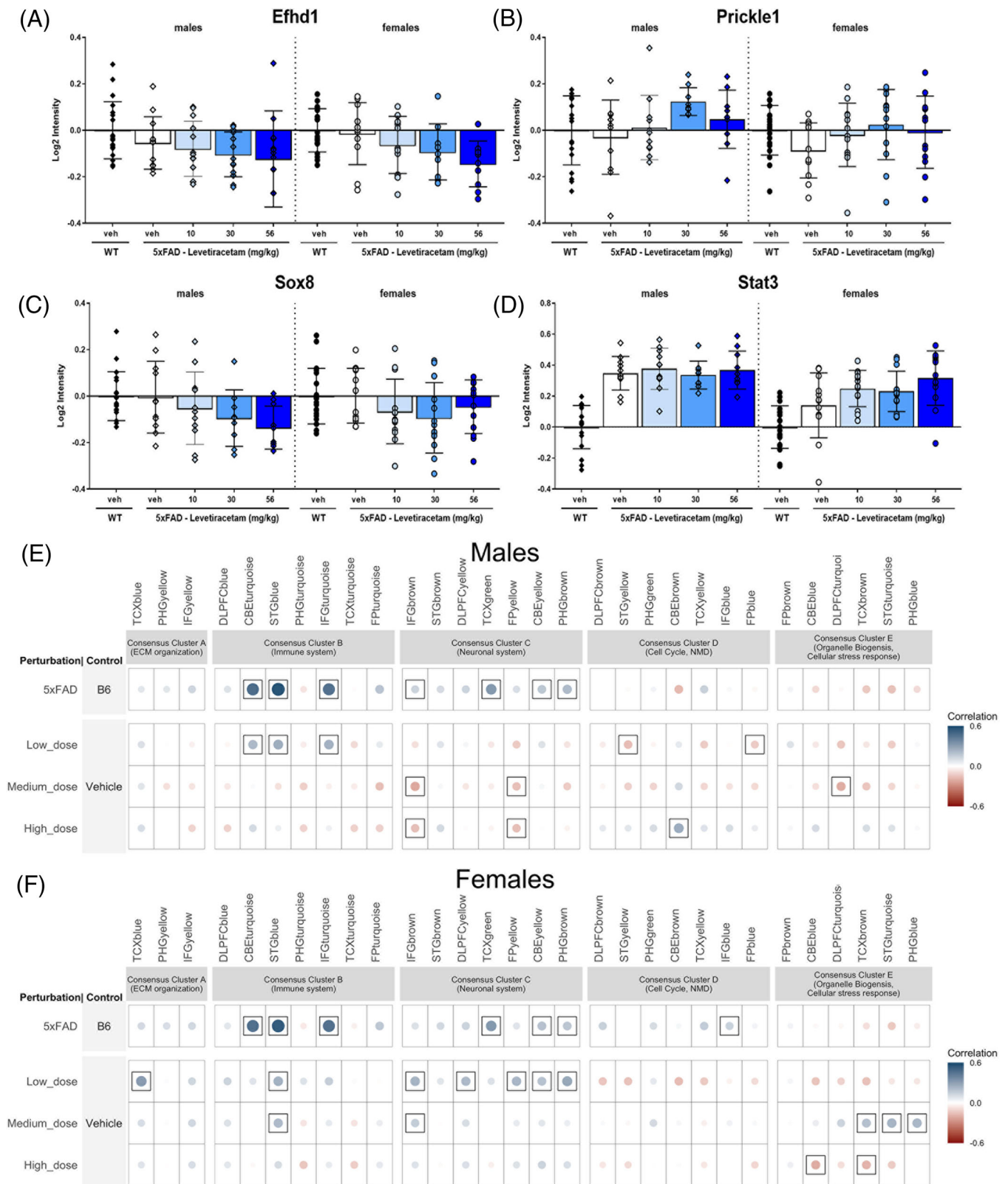


FIGURE 5 A–D, Linear regression analysis identified genes that demonstrated significant dose-related changes. Representative examples are shown here. E, F, Gene expression overlap identified by the nanoString Alzheimer's disease (AD) panel in male (E) and female (F) levetiracetam (LEV)-treated 5xFAD and human AD consensus clusters identified in Preuss et al.²⁸

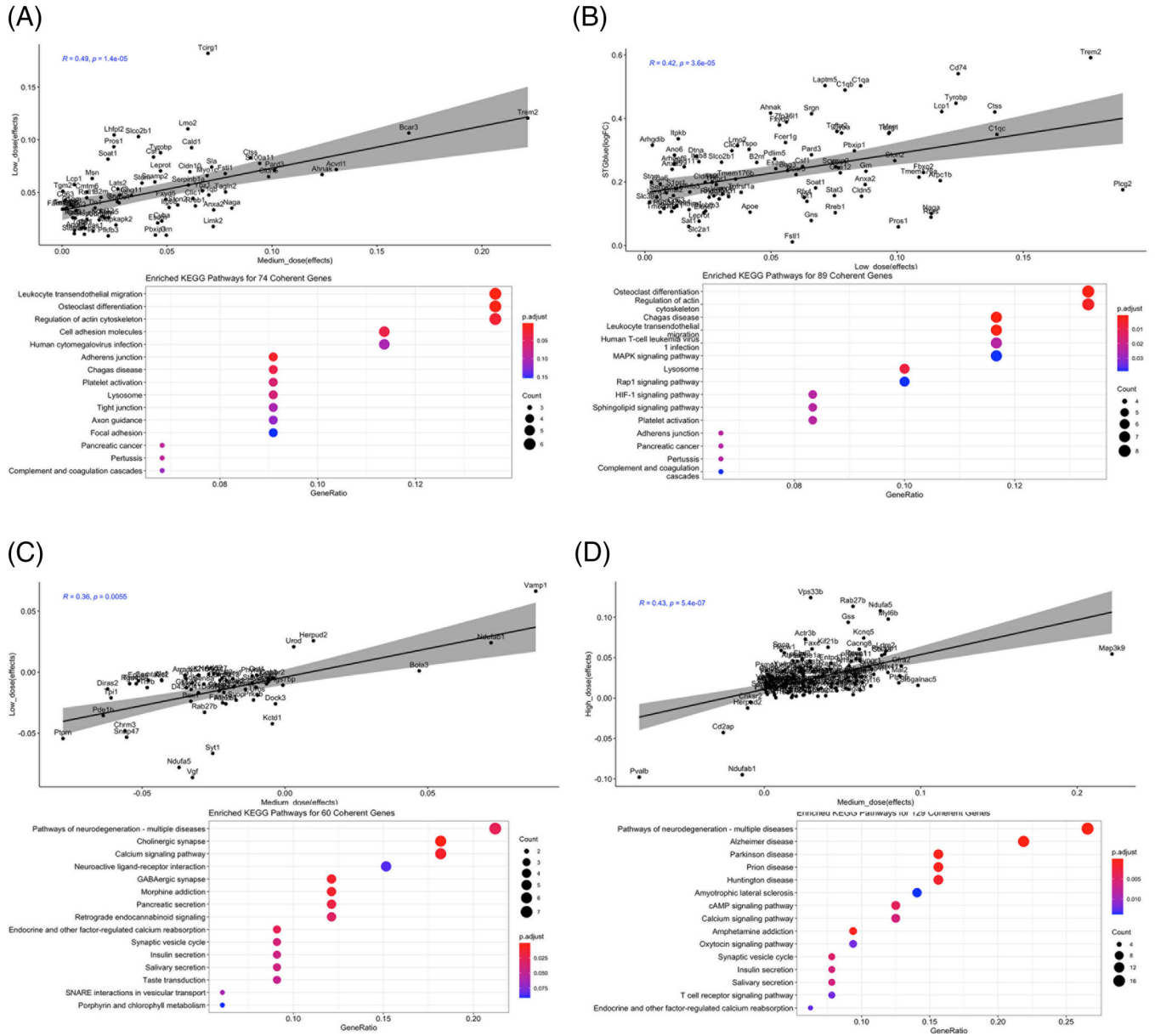


FIGURE 6 A, Dose level of levetiracetam (LEV) effects in female 5XFAD mice that were correlated with the superior temporal gyrus (STG) blue in consensus cluster B. A total of 74 coherent genes are shown between low and medium doses as there was no longer a significant correlation at the high dose (top panel). Significant Kyoto Encyclopedia of Genes and Genomes (KEGG) pathways are also shown (bottom panel). B, Dose level of LEV effects in male 5XFAD that were correlated with STG blue. There were 89 genes that were positively correlated with the low dose of LEV. C, Dose level of LEV effects in male 5XFAD that were correlated with inferior frontal gyrus (IFG) brown in consensus cluster C. While vehicle-treated mice showed a significant correlation in gene expression changes, this disappeared at the low dose and was anti-correlated for both medium and high doses of LEV. There were 60 coherent genes associated with the medium and high doses (top panel). Significant KEGG pathways are also shown (bottom panel). D, Female 5XFAD showed a similar pattern in the IFG region in gene expression as male 5XFAD. A total of 129 coherent genes were identified between medium and high doses of LEV (top panel). Significant KEGG pathways are also shown (bottom panel)

significant positive correlation with immune function disappeared in a dose-dependent manner, with the highest dose indicating there was no longer a significant correlation. The loss of correlation is indicative that human module-relevant neuroinflammation is no longer present in the LEV-treated 5XFAD. As confirmation, we performed IBA1 staining in brain sections of mice across all dose levels (Figure S4 in supporting information). The same pattern of dose-dependent changes also occurred in the neuronal system, in which the significant correlation

disappeared or became anti-correlated in a dose-dependent manner (Figure 5).

Further analyses identified the genes that were driving these significant correlations in each consensus cluster, and functional analysis was performed to determine whether the same Kyoto Encyclopedia of Genes and Genomes (KEGG) pathways were enriched across dose levels (Figure 6). For treatment-related effects that significantly correlated with the superior temporal gyrus (STG) blue module in Consensus

TABLE 2 Observed pharmacokinetics of levetiracetam after 3-month chronic PO dosing BID

	Plasma ng/mL (time = 0 h) (Mean ± SD)		Plasma ng/mL (time = 0.5 h) (Mean ± SD)		Cortex ng/g (time = 0.5 h) (Mean ± SD)	
	Female	Male	Female	Male	Female	Male
Levetiracetam						
0 mg/kg	<LOQ	<LOQ	<LOQ	<LOQ	<LOQ	<LOQ
10 mg/kg	2.50 ± 3.7	3.6 ± 6.9	6324.4 ± 2631.8	7617.6 ± 1843.7	2503.2 ± 537.9	2741.1 ± 851.6
30 mg/kg	13.8 ± 12.7	8.2 ± 9.3	21049.8 ± 4090.8	26263.8 ± 13758.7	10742.6 ± 4092.9	11821.0 ± 5109.9
56 mg/kg	10.4 ± 7.2	26.9 ± 21.8	33797.6 ± 6081.8	40161.1 ± 14832.5	20281.2 ± 5048.1	21694.3 ± 4038.3
Etiracetam						
0 mg/kg	<LOQ	<LOQ	<LOQ	<LOQ	<LOQ	<LOQ
10 mg/kg	<LOQ	<LOQ	39.3 ± 18.1	45.0 ± 8.4	23.0 ± 14.8	24.9 ± 15.1
30 mg/kg	<LOQ	<LOQ	143.9 ± 34.8	138.8 ± 41.6	73.1 ± 35.3	90.6 ± 50.9
56 mg/kg	<LOQ	<LOQ	237.8 ± 44.7	239.8 ± 52.5	150.1 ± 63.7	182.3 ± 65.0

Note: Plasma LOQ = 0.3 ng/mL; Cortex LOQ = 0.8 ng/mL.

Abbreviations: ANOVA, analysis of variance; AUC, area under the curve; BID, twice daily; LOQ, limits of quantification; PO, by mouth; SD, standard deviation.

Cluster B, 74 coherent genes were identified between the low and medium dose in females (Figure 6A). These genes included previously associated risk genes such as *Trem2*. Gene expression was enriched for KEGG pathways relevant to leukocyte transendothelial migration and osteoclast differentiation (Figure 6A). There was no significant correlation with this module at the 56 mg/kg dose. In male 5XFAD, there were 89 positively correlated (Figure 6B) and 55 negatively correlated genes with 10 mg/kg dose. Positively correlated genes were similar to those identified in females such as *Trem2* and *Plcg2*, and were enriched in KEGG pathways relevant to osteoclast differentiation and regulation of actin (Figure 6B). Negatively correlated genes such as *Axl* were enriched in the KEGG pathway relevant to tight junctions. Correlation with the STG module was no longer significant at both the 30 and 56 mg/kg doses.

Significant positive correlations ($P < .05$) also occurred in Consensus Cluster C, within the inferior frontal gyrus (IFG) brown module in a dose-related manner (Figure 5E). Vehicle-treated male 5XFAD showed a significant positive correlation ($P < .05$) in gene expression changes, which were absent after treatment with 10 mg/kg and was anti-correlated for both 30 and 56 mg/kg dose of LEV. Comparison of coherent genes between 30 and 56 mg/kg dose-identified genes such as *Map3k9* and *Cacng8* (Figure 6C). Overall, the KEGG pathways represented neurodegeneration, AD and calcium signaling, consistent with the mechanism of action of LEV.³³ Female 5XFAD showed a similar pattern in this region in both gene expression and overlap with KEGG pathways (Figure 6D), but were anti-correlated at 30 and 56 mg/kg doses.

4 | DISCUSSION

To our knowledge, this study is the first to report on the PK/PD relationship of LEV in the 5XFAD transgenic mouse model of AD. Sex differences were observed across all facets of the PK study, with C_{max} ,

$AUC_{0-\infty}$, Vd/F , and CL/F showing the greatest effects. This led to the selection of 56 mg/kg as the high dose for the chronic dosing study, as modeling of the 100 mg/kg dose predicted significant toxicity at C_{max} and large peak to trough concentrations. Comparison of predicted plasma concentrations with those observed after doses used in clinical trials with MCI patients confirmed that both the 30 and 56 mg/kg doses were above the proposed efficacious range (Figure 1E, Table 2). However, as the 5XFAD is an aggressive model of amyloidosis carrying early-onset AD mutations and demonstrates seizure activity, these higher doses were evaluated as the plasma concentrations are more in line with those used in clinical treatment of seizure activity.^{34,35} Based on the current study, and the PK/PD modeling conducted, future studies would benefit from investigation in mouse models with less severe overexpression of amyloid that may be more in line with physiologic levels. Moreover, our data also suggest that drug doses between 1 and 30 mg/kg would more closely align to plasma concentrations observed in clinical trials with MCI subjects.

Neuroimaging using ¹⁸F-AV45 showed minimal differences in amyloid deposition across LEV dose relative to vehicle treatment (Figure 2). Based on the proposed mechanism of action of LEV as a neuromodulator of synaptic transmission,^{1,7} these results were not surprising, and suggest that earlier treatment and longer duration with LEV may be required to accomplish this outcome, and are consistent with a number of preclinical studies that have used LEV in amyloid models.^{14,16,36} Functional testing revealed dose-dependent increases in hyperactivity (Figure 4), which may be indicative of potential side effect profile of LEV. However, given the therapeutic index for the dose range based on PK/PD and in consideration of the allometric scaling data, the dose range for side effects relative to the efficacious dose range may not be a major concern.

The correlation and anti-correlation of gene expression changes across doses of LEV in the mice to two human AMP AD consensus clusters was promising (Figure 5). Dose-dependent changes in gene expression relevant to the neuronal Consensus Cluster C, and over-

lap with KEGG pathways specific to synaptic signaling are consistent with the hypothesized mechanism of action of LEV.⁷ This suggests that the drug was modulating appropriate pathways, and it may be possible that starting earlier and longer treatment duration would enhance and strengthen this effect long enough for synaptic remodeling to occur.¹⁶

While it was expected that gene expression would be significantly correlated in the vehicle-treated 5XFAD in the immune Consensus Cluster B, there was a loss of this correlation with increased LEV dosing in both male and female treated animals. These data are consistent with recent work that showed that treatment with LEV in aged hAPP mice prevented aberrant microglia gene expression.³⁶ The authors suggest that epileptiform activity observed in this model influences microglia directly, and that the reduction of the microglial gene TREM2 exacerbates this activity. This is consistent with the known regulation of phagocytosis via TREM2-activation of PLCG2,^{20,21} which would result in impaired amyloid clearance in this model.

While the comparison between mouse and human transcriptomics is limited due to comparison of mouse brain hemisphere rather than with specific brain regions in the human, there were still significant correlations with LEV dose. When paired with the result of regional ¹⁸F-FDG PET, 'analogous' mouse brain regions to that of humans (STG and IFG) showed significant differences in brain glycolysis. Interestingly, these significant differences were observed in secondary motor cortex, consistent with reports of motor hyperactivity observed in open field and spontaneous alternation,³⁷ and was further exacerbated with LEV treatment in our study (Figure 4).

There are some caveats to this work worth noting. The 5XFAD mouse is not ideal, and exhibits early and severe amyloidosis, epileptiform seizures which are not fully penetrant, and lacks other critical AD features. Despite this, LEV did show significant dose-specific differences in glycolysis, and gene expression changes suggesting potential efficacy using a precision medicine approach focused on specific patient populations. Plasma concentrations observed in the current study at the middle and higher doses were above blood levels shown to be effective in human clinical trials in MCI and early-onset AD patients. Although the higher two doses administered in the present study resulted in blood levels in excess of the clinical effectiveness range, the lowest dose was effective at altering metabolism, and gene expression consistent with clinical studies. Based on this, future studies would benefit from lower dose levels, and testing in a non-transgenic LOAD model, which would more closely align the primary pathology to patient subtypes.

Overall, the present findings implicate the potential of LEV for treatment of AD for patients with impaired brain glycolysis and gene expression changes determined with treatment. These gene expression changes overlapped with specific brain region differences in humans and occurred in disease-relevant pathways. The results also highlight the importance of considering sex differences in pharmacokinetics and across all outcome measures.

ACKNOWLEDGMENTS

The authors would like to acknowledge the JAX Center for Biometric Analysis staff for assistance with chronic dosing studies and

behavioral testing. They would also like to acknowledge the JAX Genome Technologies core for assistance with RNA extractions and sample processing for NanoString. The authors also wish to thank the IU Preclinical Model Testing Core at the IU Simon Cancer Center for the generous gift of mouse brains used in the formulations development and testing. The results published here are in whole or in part based on data obtained from the AD Knowledge Portal (<https://adknowledgeportal.org>). Study data were provided by the Rush Alzheimer's Disease Center, Rush University Medical Center, Chicago. Data collection was supported through funding by NIA grants P30AG10161 (ROS), R01AG15819 (ROSMAP; genomics and RNAseq), R01AG17917 (MAP), R01AG36836 (RNAseq), the Illinois Department of Public Health (ROSMAP), and the Translational Genomics Research Institute (genomic). Additional phenotypic data can be requested at www.radc.rush.edu. Mount Sinai Brain Bank data were generated from *post mortem* brain tissue collected through the Mount Sinai VA Medical Center Brain Bank and were provided by Dr. Eric Schadt from Mount Sinai School of Medicine. The Mayo RNAseq study data was led by Dr. Nilüfer Ertekin-Taner, Mayo Clinic, Jacksonville, FL as part of the multi-PI U01 AG046139 (MPIs Golde, Ertekin-Taner, Younkin, Price). Samples were provided from the following sources: The Mayo Clinic Brain Bank. Data collection was supported through funding by NIA grants P50 AG016574, R01 AG032990, U01 AG046139, R01 AG018023, U01 AG006576, U01 AG006786, R01 AG025711, R01 AG017216, R01 AG003949, NINDS grant R01 NS080820, CurePSP Foundation, and support from Mayo Foundation. Study data include samples collected through the Sun Health Research Institute Brain and Body Donation Program of Sun City, Arizona. The Brain and Body Donation Program is supported by the National Institute of Neurological Disorders and Stroke (U24 NS072026 National Brain and Tissue Resource for Parkinsons Disease and Related Disorders), the National Institute on Aging (P30 AG19610 Arizona Alzheimer's Disease Core Center), the Arizona Department of Health Services (contract 211002, Arizona Alzheimer's Research Center), the Arizona Biomedical Research Commission (contracts 4001, 0011, 05-901 and 1001 to the Arizona Parkinson's Disease Consortium), and the Michael J. Fox Foundation for Parkinson's Research. The data for this study were funded through grant NIA U54AG054345.

CONFLICTS OF INTEREST

The authors do not report any competing interests. Author disclosures are available in the [supporting information](#).

REFERENCES

1. Kumar AM, Maini K, Kadian R. *Levetiracetam*. 2021. National Center for Biotechnology Information.
2. Bakker A, Krauss GL, Albert MS, et al. Reduction of hippocampal hyperactivity improves cognition in amnesic mild cognitive impairment. *Neuron*. 2012;74(3):467-474.
3. Lippa CF, Rosso A, Hepler M, Jenssen S, Pillai J, Irwin D. Levetiracetam: a practical option for seizure management in elderly patients with cognitive impairment. *Am J Alzheimers Dis Other Demen*. 2010;25(2):149-154.
4. AlzForum. AGB101. 2021 09/17/2021 [cited 2021 11/12/2021]; Available from: <https://www.alzforum.org/therapeutics/agb101>

5. Celone KA, Calhoun VD, Dickerson BC, et al. Alterations in memory networks in mild cognitive impairment and Alzheimer's disease: an independent component analysis. *J Neurosci*. 2006;26(40):10222-10231.
6. Tran TT, Speck CL, Pisupati A, Gallagher M, Bakker A. Increased hippocampal activation in ApoE-4 carriers and non-carriers with amnesic mild cognitive impairment. *Neuroimage Clin*. 2017;13:237-245.
7. Lynch BA, Lambeng N, Nocka K, et al. The synaptic vesicle protein SV2A is the binding site for the antiepileptic drug levetiracetam. *Proc Natl Acad Sci U S A*. 2004;101(26):9861-9866.
8. Garcia-Perez E, Mahfooz K, Covita J, Zanduetta A, Wesseling JF. Levetiracetam accelerates the onset of supply rate depression in synaptic vesicle trafficking. *Epilepsia*. 2015;56(4):535-545.
9. Bakker A, Albert MS, Krauss G, Speck CL, Gallagher M. Response of the medial temporal lobe network in amnesic mild cognitive impairment to therapeutic intervention assessed by fMRI and memory task performance. *Neuroimage Clin*. 2015;7:688-698.
10. Musaeus CS, Shafi MM, Santarnecchi E, Herman ST, Press DZ. Levetiracetam alters oscillatory connectivity in Alzheimer's disease. *J Alzheimers Dis*. 2017;58(4):1065-1076.
11. Magalhães JC, Gongora M, Vicente R, et al. The influence of levetiracetam in cognitive performance in healthy individuals: neuropsychological, behavioral and electrophysiological approach. *Clin Psychopharmacol Neurosci*. 2015;13(1):83-93.
12. Toniolo S, Sen A, Husain M. Modulation of brain hyperexcitability: potential new therapeutic approaches in Alzheimer's disease. *Int J Mol Sci*. 2020;21(23):9318.
13. Vossel KA, Ranasinghe KG, Beagle AJ, et al. Incidence and impact of subclinical epileptiform activity in Alzheimer's disease. *Ann Neurol*. 2016;80(6):858-870.
14. Klee JL, Kiliaan AJ, Lipponen A, Battaglia FP. Reduced firing rates of pyramidal cells in the frontal cortex of APP/PS1 can be restored by acute treatment with levetiracetam. *Neurobiol Aging*. 2020;96:79-86.
15. Schneider F, Baldauf K, Wetzel W, Reymann KG. Behavioral and EEG changes in male 5xFAD mice. *Physiol Behav*. 2014;135:25-33.
16. Sanchez PE, Zhu L, Verret L, et al. Levetiracetam suppresses neuronal network dysfunction and reverses synaptic and cognitive deficits in an Alzheimer's disease model. *Proc Natl Acad Sci U S A*. 2012;109(42):E2895-903.
17. Kemppainen N, Joutsa J, Johansson J, et al. Long-term interrelationship between brain metabolism and amyloid deposition in mild cognitive impairment. *J Alzheimers Dis*. 2015;48(1):123-133.
18. Huijbers W, Mormino EC, Schultz AP, et al. Amyloid-beta deposition in mild cognitive impairment is associated with increased hippocampal activity, atrophy and clinical progression. *Brain*. 2015;138(Pt 4):1023-1035.
19. Hector A, Brouillette J. Hyperactivity induced by soluble amyloid-beta oligomers in the early stages of Alzheimer's disease. *Front Mol Neurosci*. 2020;13:600084.
20. Sudom A, Talreja S, Danao J, et al. Molecular basis for the loss-of-function effects of the Alzheimer's disease-associated R47H variant of the immune receptor TREM2. *J Biol Chem*. 2018;293(32):12634-12646.
21. Konishi H, Kiyama H. Microglial TREM2/DAP12 signaling: a double-edged sword in neural diseases. *Front Cell Neurosci*. 2018;12:206.
22. Cavanaugh JE, Neath AA. The Akaike information criterion: background, derivation, properties, application, interpretation, and refinements. *WIREs Comput Stat*. 2019;11(3).
23. Soetaert K, Petzoldt T, Setzer RW. Solving differential equations in R: package deSolve. *J Stat Softw*. 2010;33(9):1-25.
24. R Core Team. R: a language and environment for statistical computing. 2021.
25. Percie Du Sert N, Ahluwalia A, Alam S, et al. Reporting animal research: explanation and elaboration for the ARRIVE guidelines 2.0. *PLoS Biol*. 2020;18(7):e3000411.
26. AGB101.
27. Oblak AL, Lin PB, Kotredes KP, et al. Comprehensive evaluation of the 5XFAD mouse model for preclinical testing applications: a MODEL-AD study. *Front Aging Neurosci*. 2021;13:713726.
28. Preuss C, Pandey R, Piazza E, et al. A novel systems biology approach to evaluate mouse models of late-onset Alzheimer's disease. *Mol Neurodegener*. 2020;15(1):67.
29. Mostafavi S, Gaiteri C, Sullivan SE, et al. A molecular network of the aging human brain provides insights into the pathology and cognitive decline of Alzheimer's disease. *Nat Neurosci*. 2018;21(6):811-819.
30. Allen M, Carrasquillo MM, Funk C, et al. Human whole genome genotype and transcriptome data for Alzheimer's and other neurodegenerative diseases. *Sci Data*. 2016;3:160089.
31. Wang M, Beckmann ND, Roussos P, et al. The Mount Sinai cohort of large-scale genomic, transcriptomic and proteomic data in Alzheimer's disease. *Sci Data*. 2018;5:180185.
32. Wan Y-W, Al-Ouran R, Mangleburg CG, et al. Meta-analysis of the Alzheimer's disease human brain transcriptome and functional dissection in mouse models. *Cell Rep*. 2020;32(2):107908.
33. Dubovsky SL, Daurignac E, Leonard KE, Serotte JC. Levetiracetam, calcium antagonism, and bipolar disorder. *J Clin Psychopharmacol*. 2015;35(4):422-427.
34. Cumbo E, Ligor LD. Levetiracetam, lamotrigine, and phenobarbital in patients with epileptic seizures and Alzheimer's disease. *Epilepsy Behav*. 2010;17(4):461-466.
35. Liu J, Wang LN, Wu LY, Wang YP. Treatment of epilepsy for people with Alzheimer's disease. *Cochrane Database Syst Rev*. 2016;11:CD011922.
36. Das M, Mao W, Shao E, et al. Interdependence of neural network dysfunction and microglial alterations in Alzheimer's disease-related models. *iScience*. 2021;24(11):103245.
37. Sukoff Rizzo SJ, Anderson LC, Green TL, MCGarr T, Wells G, Winter SS. Assessing healthspan and lifespan measures in aging mice: optimization of testing protocols, replicability, and rater reliability. *Curr Protoc Mouse Biol*. 2018;8(2):e45.

SUPPORTING INFORMATION

Additional supporting information can be found online in the Supporting Information section at the end of this article.

How to cite this article: Onos KD, Quinney SK, Jones DR, et al. Pharmacokinetic, pharmacodynamic, and transcriptomic analysis of chronic levetiracetam treatment in 5XFAD mice: A MODEL-AD preclinical testing core study. *Alzheimer's Dement*. 2022;8:e12329. <https://doi.org/10.1002/trc2.12329>